

## ***Interactive comment on “Cloud and aerosol radiative effects as key players for anthropogenic changes in atmospheric dynamics over southernWest Africa” by Konrad Deetz et al.***

**Konrad Deetz et al.**

konrad.deetz@kit.edu

Received and published: 19 June 2018

Answer to Referee #1 Konrad Deetz 19 June 2018

Dear Referee (Atmospheric Chemistry and Physics),

thank you for your report from 13 April 2018. We have accounted for the comments and suggestions in the revised manuscript version. Please find our replies (marked with #) to the individual comments in the following. Before the detailed replies to your comments we want to stress one important overarching point: This study mainly focuses on the sensitivity of atmospheric dynamics and cloud properties to aerosols and not on a

C1

detailed validation of the model system. Nevertheless, we have done a comprehensive evaluation of the model with the available observations of the DACCIIWA measurement campaign. We show corresponding figures in our replies which appear at the end of this document. (The complete figure captions are given within the text because the figure caption space for the uploaded figures is not sufficient.)

Sincerely, Konrad Deetz on behalf of all coauthors

Referee comments:

(0) The authors analyze six simulations of the COSMO-ART regional model with an outer domain of roughly 40 x 40 degrees centered around the Bight of Benin and an inner domain of roughly 10 x 15 degrees aligned along the Gold Coast of Southern West Africa. A main strength of the study is that the authors conduct an extensive analysis of the simulations to suss out patterns of response to aerosol conditions, and to draw some conclusions about some mechanisms and hypotheses about others. A main weakness of the study is that almost no comparisons to observations are made nor are the realism of assumed meteorological or surface or aerosol properties discussed, leaving the reader necessarily uncertain as to the degree to which the simulations are basically realistic, either in the baseline state or in the dynamic range of aerosol conditions investigated. Especially in today's satellite age, it should not be considered a sufficient evaluation of a regional model simulation to compare results only to droplet number concentration observations. Based on the simulations, the authors advance a schematic diagram of how near-coastal meteorological conditions could be impacted by increasing regional pollution during the monsoonal period when no land-sea breeze period occurs. Observational work, for instance using satellite observations, would be required to confirm the robustness of the proposed mechanism and its strength for a given dynamic range of aerosol relative to other regional-scale drivers that are held fixed in the current study, such as sea surface temperature.

# The high resolution realizations with COSMO-ART are computational expensive and

C2

therefore we had to restrict to a short time period. We commonly agreed on the 3-4 July 2016 as a golden day due to the intensive stratus period observed over Savè (Kalthoff et al., 2018). The data analysis of the COSMO-ART results revealed that the AI is most pronounced and coherent over Ivory Coast (Figure 5 in the manuscript). Therefore, we decided to focus on this area although we are aware of the fact, that the DACCIIWA measurement campaign with its supersites and aircraft operations focus more on the eastern part of the domain. For 3-4 July, no aircraft observations are available for the coastal region of Ivory Coast. Furthermore, a detailed assessment of the MODIS AOD data revealed that the data availability over SWA (land area) is substantially reduced by the presence of clouds (see Review-Figure 6). Nevertheless, we comprehensively evaluated COSMO-ART in (a) past studies and also (b) within DACCIIWA for SWA. (a) The full capacity of COSMO-ART was applied in numerous studies. Knöbe et al. (2011) validated the aerosol and gaseous compounds in detail against observations for the European area. Stanelle et al. (2010) analyzed the ADE of mineral dust over the Sahara that alters the near-surface temperature up to 4 K in case of elevated mineral dust layers. Furthermore, feedbacks between the mineral dust ADE and the atmospheric dynamics lead to modifications in the mineral dust emission. Athanasopoulou et al. (2014) quantified a severe wildfire event over Greece in 2007 in terms of air quality and ADE that reveals AOD values between 0.75 and 1 and a cooling of 0.5 K. Walter et al. (2016) extended COSMO-ART with a plume-rise model to describe biomass burning pollution injection heights and applied the model to Canadian forest fires in 2010. The ADE related to the biomass burning plume leads to a near-surface cooling of up to 6 K. The ADE of sea salt over the Mediterranean Sea, Northeast Atlantic, North Sea and Baltic Sea was modeled by Lundgren et al. (2013) in accordance to the observations from remote sensing. Kraut (2015) applied an ensemble approach by including random temperature perturbations to isolate the sea salt AIE on the characteristics of a cyclone over the Mediterranean Sea in 2011, revealing spatial shifts and intensity differences in the precipitation patterns. By considering the AIE on post-frontal convective clouds over Germany in 2008, the cloud properties were changed significantly, leading to a

C3

reduction in precipitation with increasing aerosol amounts (Rieger et al., 2014). (b) In the preparation of the high resolution process study simulations with COSMO-ART for SWA, we conducted operational forecasts for the area over the time period 8 March to 31 July with a grid mesh size of 28 km. This allows us to comprehensively analyze the model performance with respect to meteorology and air pollution and to prepare reasonable COSMO-ART data for the nesting of our high resolution realizations. Also we found tendencies of overestimations of trace gas concentrations in COSMO-ART, likely due to uncertainties in the emission inventories, COSMO-ART reasonably reproduces the SWA meteorological and air pollution characteristics. To support these findings and to meet the concerns of the reviewer, the following 7 figures are attached to this review answer:

- Review-Figure-1: Temporal evolution of the height (m AGL) of the wind speed maximum between 0 and 1500 m AGL for the mean 57 h forecast lead time. (13 June - 30 July 2016) at Savè as observed (black, Doppler Lidar) and modeled with COSMO-ART (blue). The shaded areas denote the standard deviation.

- Review-Figure-2: Wind speed profile (m s<sup>-1</sup>) between 0 and 2000 m ASL as mean diurnal cycle (13 June - 30 July 2016) at Savè for (a) COSMO-ART and (b) Doppler Lidar observation.

- Review-Figure-3: Vertical profiles (km AGL) of BC (mg m<sup>-3</sup>) at Savè for (a-c) 5 July 2016, (d-g) 14 July 2016 and (h-i) 15 July 2016. The ALADINA (small unmanned aircraft) observations of total BC are denoted in black, the COSMO-ART results for fresh BC, aged BC (Aitken mode), aged BC (accumulation mode) and total BC are shown in green, blue, brown and red, respectively. The observations were temporally assigned to the 3 hourly model output with a deviation not greater than 1 hour and by subsequently interpolating the model data to the ALADINA altitudes. Within these time steps, ALADINA conduct several ascends and descends. It is assumed that the observations within the time steps are measured instantaneously and the data is sorted according to their altitude, to allow for clearness of the visualization.

C4

- Review-Figure-4: Comparison of Twin Otter measurement flight TO-16 (14 July 2016, 06:44 UTC to 09:50 UTC) results with COSMO-ART. For a comparison the model output of 9 UTC and the measurements 15 minutes around this time step (08:45-09:15 UTC) were selected. (a) Flight altitude (m AGL), (b) flight track, (c) NO<sub>x</sub> concentration (ppbv) at 750m height and flight track, (d) vertical transect of NO<sub>x</sub> concentration (ppbv) along the flight track with aircraft observations included, (e) temperature (°C), (f) specific humidity (kg kg<sup>-1</sup>), (g) CO concentration (ppbv), (h) NO concentration (ppbv), (i) NO<sub>2</sub> concentration (ppbv), (j) NO<sub>x</sub> concentration, (k) O<sub>3</sub> concentration (ppbv) and (l) SO<sub>2</sub> concentration (ppbv). The panels (e)-(l) present the COSMOART results in blue and the observations in black. The horizontal color lines on top of these panels are denoted to the colors in panel (a) and (b) to illustrate the aircraft location related to the observed trace gas concentrations.

- Review-Figure-5: Mean total AOD averaged from 27 June to 17 July 2016 of (a) COSMO-ART, spatiotemporally collocated with MODIS Terra, (b) MODIS Terra, (c) COSMO-ART, collocated spatiotemporally with MODIS Aqua and (d) MODIS Aqua.

- Review-Figure-6: Number of observations within the time period 27 June - 17 July of (a) MODIS Terra and (b) MODIS Aqua

- Review-Figure-7: AOD (550 nm) at Savè from COSMO-ART (blue), CAMS (green) and AERONET (red) between 13 June - 31 July 2016 for (a) mineral dust, (b) sea salt, (c) anthropogenic aerosol and (d) total aerosol. Consider the different scaling of the ordinates. Data gaps are related to technical issues during the forecast.

Further intercomparison between COSMO-ART and observations obtained within DACCIWA including the supersites and aircraft, other models or remote sensing data is summarized in Section 5 of (<https://publikationen.bibliothek.kit.edu/1000077925>). However, we have not added the evaluation material since it would distract from the main purpose of the study to disentangle potential effects from aerosol on AI and SCT in a sensitivity study. Nevertheless, we agree that the paper also has to show that it

C5

is generally able to reasonably reproduce the conditions in SWA. To account for your comment, we added an intercomparison of the shortwave, longwave, sensible and latent heat flux with observations at Save supersite in Appendix A and adapted Section 2.2 (Observational data) as follows:

"Within the DACCIWA project, an extensive field campaign took place in June–July 2016 in SWA (Fig. 1b) (Flamant et al., 2018). The time period was selected to capture the onset of the WAM and a period characterized by increased cloudiness. The DACCIWA ground-based measurement campaign encompassed the time period from 13 June to 31 July 2016, including the three supersites Kumasi (Ghana), Savè (Benin) and Ile-Ife (Nigeria) (red dots in Fig. 1b). A complete overview of the DACCIWA ground-based measurement campaign, their supersites, instrumentation and a first insight into the available data is presented in Kalthoff et al. (2018). The DACCIWA airborne measurement campaign captured the time period from 27 June to 17 July 2016 (Flamant et al., 2018). The focus of this study is on Ivory Coast and therefore less observational data from the DACCIWA campaign is available for evaluation. However, a substantial evaluation with respect to meteorology and air pollution is realized with COSMO-ART over SWA with respect to other time periods and by focusing on the eastern part of the research area (not shown). This is presented in Deetz (2018). For this study, observations of the liquid cloud properties from the CDP-100 (Cloud droplet probe, data revision 3) of the British Antarctic Survey (BAS) Twin Otter aircraft on 3 July 2016 are used for a comparison with COSMO-ART. The CDP-100 is a wing mounted canister instrument including a forward-scatter optical system to measure the cloud droplet spectrum between 2-50  $\mu\text{m}$  with a frequency of 1 Hz. Additionally, the comparison of the modeled net downward shortwave and longwave radiation as well as the sensible and latent heat flux with Savè supersite is presented in Figure 17 of Appendix B. COSMO-ART reasonably reproduces the fluxes with lower fluxes with increasing aerosol as expected."

Furthermore, we added an intercomparison between COSMO-ART and the ATR42

C6

SAFIRE aircraft with respect to the aerosol number density. However, this evaluation focuses on the Lomé-Savè area and not on Ivory Coast (since for this date no observations for Ivory Coast are available). In Section 2.2 (Observational data) we added the following text: "The aerosol aerosol number density is evaluated using observations of the ATR42 SAFIRE (Service des Avions Français 25 Instrumentés pour la Recherche en Environnement) for the 3 July 2016. Additionally, the comparison of the modeled net downward shortwave and longwave radiation as well as the sensible and latent heat flux with Savè supersite is presented in Figure 19 of Appendix B. COSMO-ART reasonably reproduces the fluxes with lower fluxes with increasing aerosol as expected." In Section 4 (Evaluation of modeled cloud and aerosol properties with aircraft observations) we added the following text: "The research aircraft ATR42 SAFIRE also obtained aerosol properties in the Lomé-Savè area on 3 July 2016 (8:32–13:16 UTC). The flight track and altitude is presented in Figure 5, showing similar flight patterns compared to the Twin Otter (Fig. 3). By assuming dry aerosol, Figure 6 shows the comparison between COSMO-ART and the Spectrometer Scanning Mobility Particle Sizer (SMPS) to evaluate the Aerosol Number Density in the size range 0.02–0.5  $\mu\text{m}$ . Figure 6 reveals that the modeled aerosol number density shows a similar temporal evolution compared to the observations but has a constant bias, overestimating the observed aerosol number density by a factor of about 2 (indicated by the blue dashed line). Therefore, in the subsequent study it has to be considered that the reference case shows already higher aerosol concentrations compared to the current state in SWA as quantified by the aircraft measurements. Overall, the evaluation reveals that COSMO-ART is capable to reproduce the aerosol situation on 3 July 2016 over SWA which is the basis for further sensitivity studies.

The figures related to this passage are attached in this review answer:

Fig.5 -> Review-Figure-8: Flight track of the ATR42 SAFIRE on 3 July 2016 between 08:32 UTC and 13:13 UTC in (a) horizontal and (b) vertical dimension (m AGL). For (a) the topography (m ASL) is added. The flight track in (a) and (b) is separated in hourly

C7

time steps for the subsequent collocation with hourly model data from COSMO-ART, highlighted by the pink (08:32–09:30 UTC), blue (09:30–10:30 UTC), gray (10:30–11:30 UTC), red (11:30–12:30 UTC) and black color (12:30–13:13 UTC). Furthermore, the arrows in (a) indicate the flight direction with the takeoff at Lomé, the flight to Savè and the return to Lomé airport. Shortly. Note the meridional compression of the map in (a).

Fig.6 -> Review-Figure-9: Aerosol number density (AND,  $\text{cm}^{-3}$ ) in the size interval 0.02 to 0.5  $\mu\text{m}$  as measured by the Spectrometer Scanning Mobility Particle Sizer (SMPS) on board the ATR42 (black) and modeled with COSMO-ART (solid blue, reference case). The horizontal dashed blue line shows the COSMO-ART AND divided by 2. The vertical blue dashed lines indicate the COSMO-ART model output hours, which are compared to the observations.

Fig. 19 (Appendix B) -> Review-Figure-10: Comparison between Savè supersite observations (grey) and COSMO-ART reference (black), clean (blue) and polluted (red) of (a) net downward shortwave radiation ( $\text{W m}^{-2}$ ), (b) net downward longwave radiation ( $\text{W m}^{-2}$ ), sensible heat flux ( $\text{W m}^{-2}$ ) and latent heat flux ( $\text{W m}^{-2}$ ). The horizontal lines in (a) denote clouds over Savè in the observations and COSMO-ART.

You mentioned that the study does not explicitly exclude the land sea-breeze but land sea-breeze effects can hardly be disentangled from AI effects because the monsoon flow superimposes the land-sea breeze. The conclusion of the manuscript closes with the suggestion of ideas to assess the aerosol-AI impact via observation. We proposed: "A potential strategy is the analysis of the AI front around noon via remote sensing cloud observations from past to present by assuming a positive trend in the aerosol burden. It is expected that the daytime AI front location has shifted landwards from the past to current conditions but also other phenomena (e.g. decadal SST variations) have the potential to affect the front location." This assessment is suitable for a companion paper but is clearly beyond the scope of this paper.

C8

(1) In the introduction the authors refer twice to "convective-cloud invigoration mechanism," the first time apparently referring to cold clouds and the second time to warm clouds (page 2, line 32). Is this the same mechanism? Please clarify in the text to what degree the mechanism being referred to operates in simulations and under what conditions, versus established in observations and under what conditions.

# Saleeby et al. (2014) show that the convective-cloud invigoration mechanism is not restricted to cold clouds. Also in warm cumuliform clouds, the enhanced condensation under polluted conditions can lead to further release of latent heat, intensified upward motion and therefore to more clouds. This is considered by the model. I don't see your point. Could you please explain more in detail what do you expect?

(2) The six simulations vary only aerosol mass and number concentrations, but how this is done is not described. The authors state that the mass and number are scaled by factors of 0.1, 0.25, 0.5, 1, 2 and 4. Since there is "aerosol-chemistry spin up" the only way I can understand this is if the values are scaled only when some process rates are calculated, but which process rates? Please clarify in the text.

# Generally, the aerosol amount during the whole simulation period is not changed. Just when it comes to the calculation of the radiative transfer (in case of ADE) and the aerosol activation (AIE) the aerosol mass and number is scaled. We clarified it in the text (Section 2.1): "Note, that the aerosol scaling only comes into consideration when deriving the aerosol optical properties (with respect to ADE) and the aerosol activation (with respect AIE). All aerosol dynamic processes remain unaffected by the scaling."

(3) Please report aerosol properties that correspond to the simulations somehow in Table 1 or similar format. Did the aircraft campaign for this special issue make any aerosol measurements at all that are relevant for comparison? Can the simulated aerosol conditions be compared somehow and somewhere to measurements? I consider it mandatory to indicate in the manuscript in quantitative terms (beyond a multiplicative factor) what is the dynamic range considered in this study in terms of basic

C9

measurable units such as CN, CCN, AOD, PM1, PM2.5 or the like.

# Refers to (0). Furthermore we added a plot to quantify the aerosol change that is related to the aerosol scaling: - Review-Figure-11: Temporal evolution of median (a) total aerosol number (cm<sup>-3</sup>) and (b) total aerosol mass (μg m<sup>-3</sup>) in the lowest 2 km AGL over Ivory Coast (7.5–3.0°W) between 2 July 15 UTC to 3 July 21 UTC for the clean (blue dashed), reference (black solid) and polluted case (red solid), based on the aerosol scaling introduced in Table 1.

(4) Owing to the leading role of direct effect, simulated single-scattering albedo should be somehow quantitatively reported from simulated values and compared to measurements or other at a minimum reported simulations somewhere relevant in Africa.

# The SSA is calculated in COSMO-ART to derive the aerosol effect on radiation. However, the SSA is not a standard output variable and therefore is not available for a comparison with observations. As far as we know, SSA observations are not available within DACCIWA except of AERONET. AERONET has three relevant stations: KITcube Save, Ilorin and Koforidua. They provide the SSA but only in four discrete wavelength. COSMO-ART uses wavebands (intervals) so a direct comparison is not possible. To focus only on the time period 2-3 July 2016, as done in this study, allows no robust evaluation. The comparison of modeled and observed AOD is compared with AERONET and the CAMS model in Review-Figure-7 for a longer period. It supports our finding that the anthropogenic aerosol is overestimated in COSMO-ART likely due to the uncertainty in the emission inventories.

(5) The authors seem to focus on sensible heat flux without considering the role of soil moisture and latent heat flux (e.g., in the abstract and conceptual diagram). Is latent heat flux irrelevant at this location? Also at locations of previous studies? I have to assume that precipitation within the inner domain is negligible during the monsoon season and the surface starts out very dry, but that is not stated (please clarify in the text).

C10

# We agree on that and added the consideration of the latent heat flux in the text. According to that the latent heat flux curve is added in Figure 13 of the manuscript. See Review-Figure-12.

(6) Please clarify in the text how soil moisture is initialized in the simulations, whether results are sensitive to how that is done.

# Since we focus on short time periods in the order of days, the COSMO-ART realizations are performed in NWP mode, the soil moisture is initialized via the meteorological boundary conditions of ICON. Therefore there is no long-term spinup of soil moisture as it is done for climate projections e.g. when using the CLM version of COSMO. NLLS is not related to significant amounts of precipitation (sporadic drizzle) and is therefore not altering the soil moisture. We expect that the cool and moist air, advected with AI, dominates the meteorological characteristics as presented in Figure 6. We agree that soil moisture is worth to focus on, when we talk about the onset of convection in the afternoon. However, the sensitivity of soil moisture on the aerosol-AI interactions is beyond the scope of our study. The soil moisture is also important when parameterizing the emission of mineral dust particles. In Deetz et al. (2016) I have shown that the soil moisture has significant impact on the mineral dust emission in Northeastern Germany. But for this SWA case study, the mineral dust contribution (primarily coming from the Sahara) is small and in this arid region the sensitivity towards soil moisture is of less importance than for central Europe.

(7) Please report whether simulations are sensitive to other factors, including inner or outer domain locations or sizes, grid mesh resolution, and boundary layer turbulence or cloud schemes.

# As described in the answer to comment (0), we have conducted operational forecasts with COSMO-ART from 8 March to 31 July 2016 with a grid mesh size of 28 km and a large domain capturing wide areas of Africa (25W-40E,20S-35N). It reveals that this coarse setup including parameterized convection shows deficiencies in the

C11

representation of the SWA meteorological conditions. The precipitation forecasts show less discriminance and incoming shortwave radiation and 2 m temperature are underestimated compared to Save observations. Therefore we decided not to use this data as boundary data for the nesting. We performed tests with a higher grid mesh size of 5 km, used explicit and parameterized convection, different turbulence closures available in COSMO and also tested it with and without the two-moment microphysics scheme. It turned out that by using the two-moment microphysics scheme and explicit convection best results are achieved with significant improvement towards the 28 km simulation (see attached Review-Figure-8 to Review-Figure-10, with 28 km grid mesh size (D1, blue) and 5 km (D2, green)) with Save supersite observations (black lines) as a reference.

- Review-Figure-13: Temporal evolution of the surface net downward shortwave radiation ( $W m^{-2}$ ) for the nine-day spin-up time (25 June - 3 July 2016) at Savè as observed (black, Energy Balance Station) and modeled with COSMO-ART (D1 in blue and D2 in green).

- Review-Figure-14: Temporal evolution of the 2 m temperature ( $^{\circ}C$ ) for the nine-day spin-up time (25 June - 3 July 2016) at Savè as observed (black, Energy Balance Station) and modeled with COSMO-ART (D1 in blue and D2 in green).

- Review-Figure-15: Temporal evolution of the 2 m relative humidity (%) for the nine-day spin-up time (25 June - 3 July 2016) at Savè as observed (black, Energy Balance Station) and modeled with COSMO-ART (D1 in blue and D2 in green).

Within this assessment, the turbulence closure had less impact on the results than the treatment of the convection. Therefore we used this 5 km COSMO-ART realization for the nesting simulations with 2,5 km grid mesh size.

(8) page 2, line 19: "react" → "are" or other fix

# We have changed the manuscript accordingly.

C12

(9) page 3, line 1: "dependent" -> "dependence" or other fix

# We have changed the manuscript accordingly.

(10) recommend to divide section 5 text up from one long paragraph currently

# We agree on that and subdivided Section 5 in five paragraphs.

(11) recommend to guide the reader more graphically in following the transition from figure 2 (schematic diurnal cycle) to later figures (all in UTC), such as by indicating UTC time range on the panels of figure 2

# We agree on that and added the approximated UTC time range in the caption of Figure 2. Nevertheless, it has to be noted that this is just a rough estimation. Kalthoff et al. (2018) show that the onset and the evolution of the NLLS can vary considerably from day to day and from one site to another.

Additional References Deetz, K.: Assessing the Aerosol Impact on Southern West African Clouds and Atmospheric Dynamics, Dissertation, KIT Scientific Publishing, Karlsruhe, 75, 2018.

Deetz, K., Klose, M., Kirchner, I., and Cubasch, U.: Numerical simulation of a dust event in northeastern Germany with a new dust emission scheme in COSMO-ART, Atmos. Environ., 126, 87–97, 2016.

Interactive comment on Atmos. Chem. Phys. Discuss., <https://doi.org/10.5194/acp-2018-186>, 2018.

C13

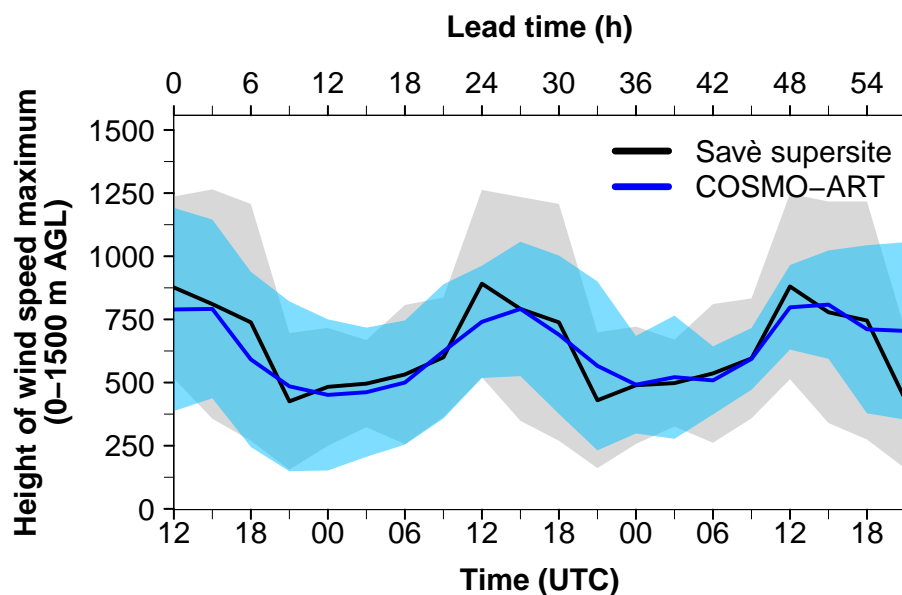


**Fig. 1.** Review-Figure-1: Temporal evolution of the height (m AGL) of the wind speed maximum between 0 and 1500 m AGL for the mean 57 h forecast lead time. (13 June - 30 July 2016) at Savè.

C14

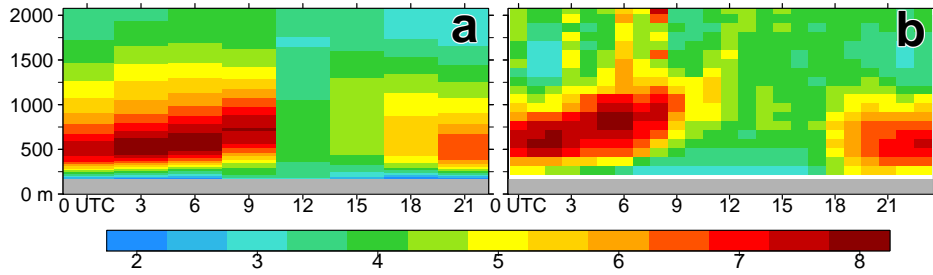


**Fig. 2.** Review-Figure-2: Wind speed profile ( $\text{m s}^{-1}$ ) between 0 and 2000 m ASL as mean diurnal cycle (13 June - 30 July 2016) at Savè for (a) COSMO-ART and (b) Doppler Lidar observation.

C15

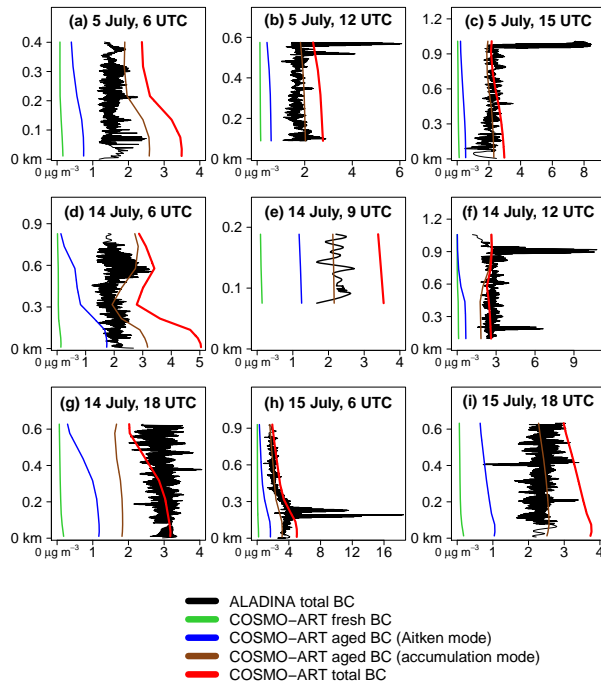


**Fig. 3.** Review-Figure-3: Vertical profiles (km AGL) of BC ( $\text{mg m}^{-3}$ ) at Savè for (a-c) 5 July 2016, (d-g) 14 July 2016 and (h-i) 15 July 2016.

C16

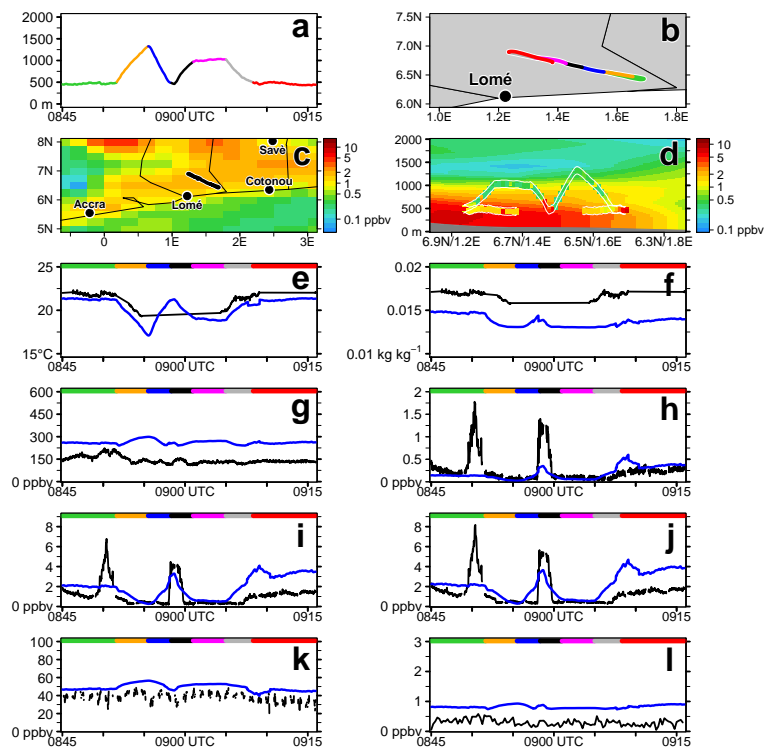


**Fig. 4.** Review-Figure-4: Comparison of Twin Otter measurement flight TO-16 (14 July 2016, 06:44 UTC to 09:50 UTC) results with COSMO-ART.

C17

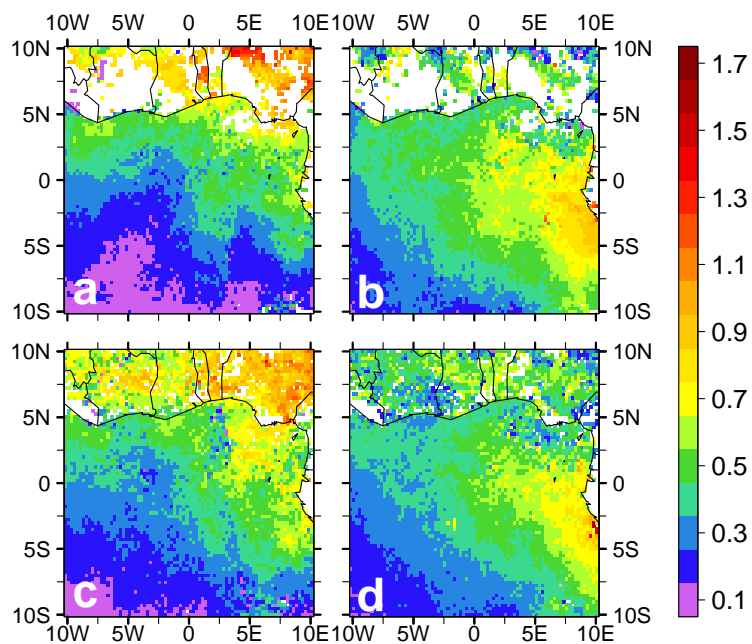


**Fig. 5.** Review-Figure-5: Mean total AOD averaged from 27 June to 17 July 2016 of (a) COSMO-ART collocated with MODIS Terra, (b) MODIS Terra, (c) COSMO-ART, collocated spatiotemporally with

C18

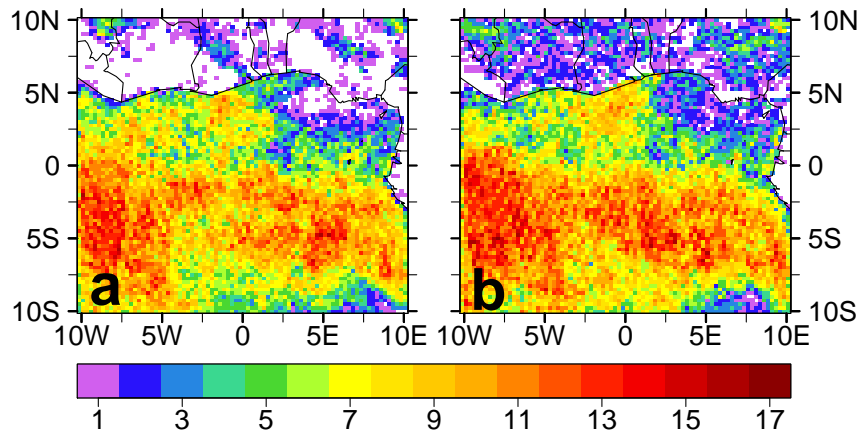


**Fig. 6.** Review-Figure-6: Number of observations within the time period 27 June - 17 July of (a) MODIS Terra and (b) MODIS Aqua.

C19

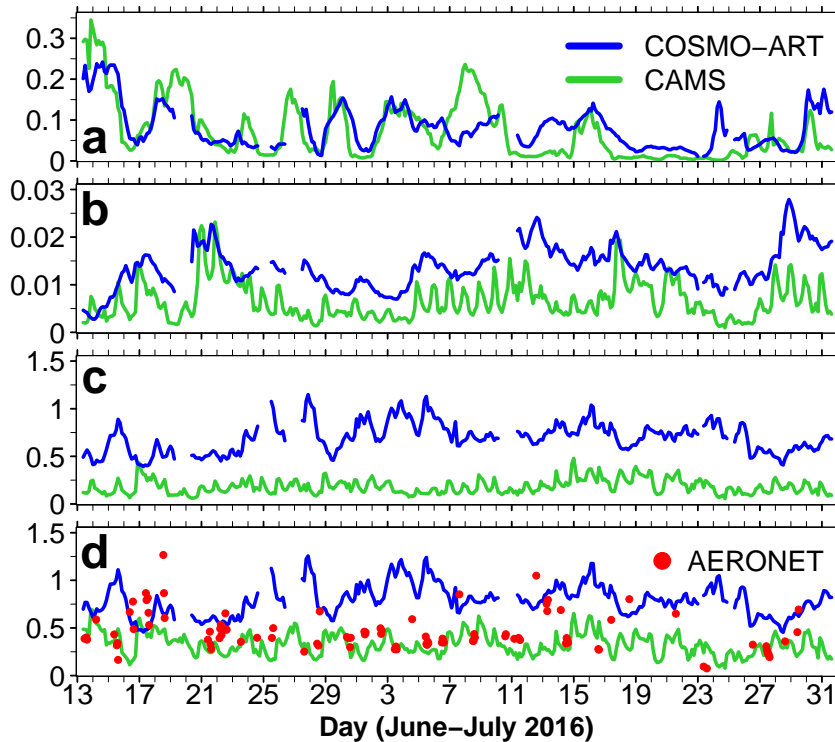


**Fig. 7.** Review-Figure-7: AOD (550 nm) at Savè from COSMO-ART (blue), CAMS (green) and AERONET (red) between 13 June - 31 July 2016 for (a) mineral dust, (b) sea salt, (c) anthropogenic aerosol and (d) total

C20

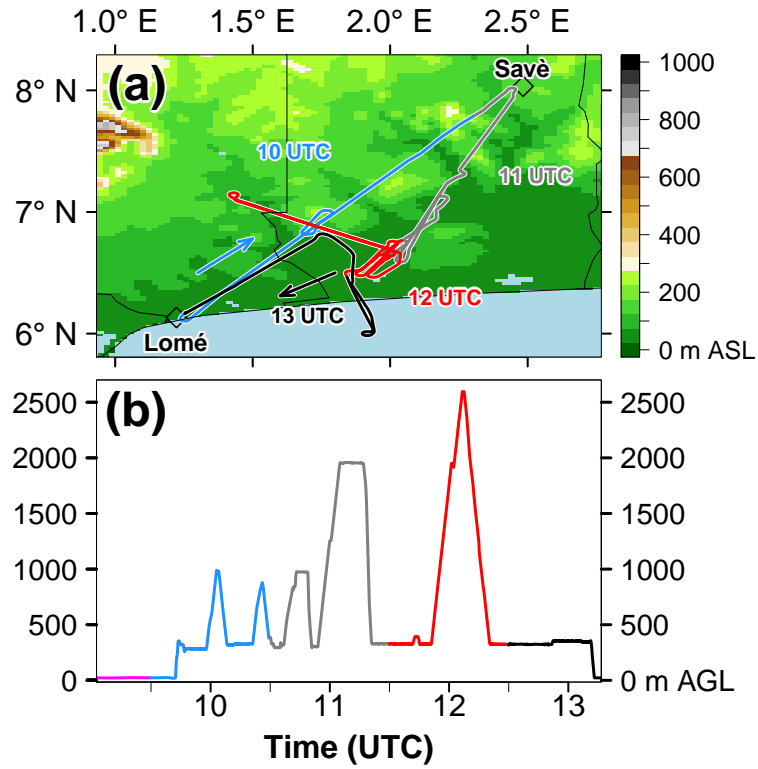


**Fig. 8.** Review-Figure-8: Flight track of the ATR42 SAFIRE on 3 July 2016 between 08:32 UTC and 13:13 UTC in (a) horizontal and (b) vertical dimension (m AGL). For (a) the topography (m ASL) is added. The flight

C21

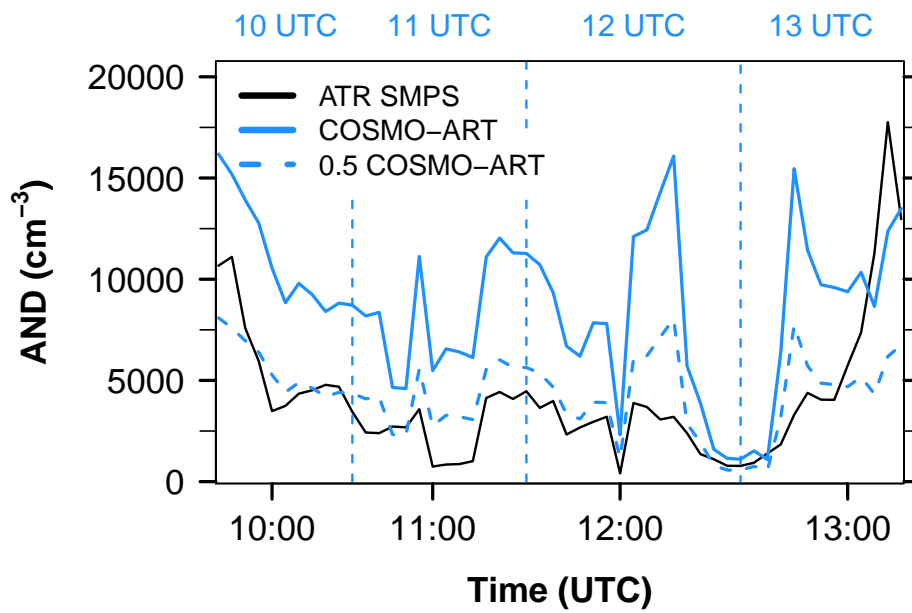


**Fig. 9.** Review-Figure-9: Aerosol number density (AND,  $\text{cm}^{-3}$ ) in the size interval 0.02 to 0.5  $\mu\text{m}$  as measured by the Spectrometer Scanning Mobility Particle Sizer (SMPS) on board the ATR42 (black) and modeled

C22

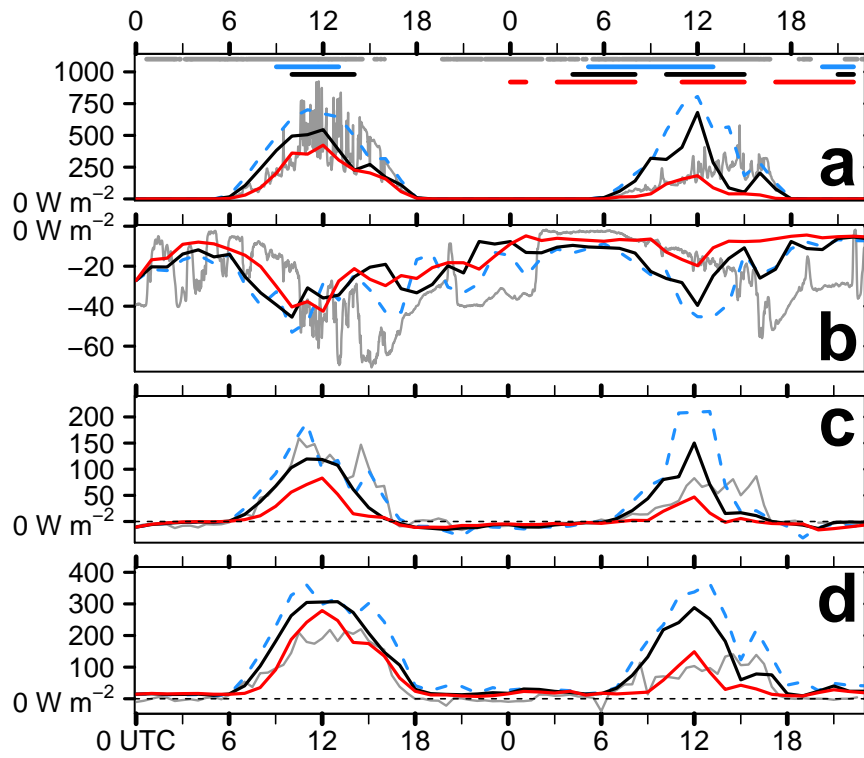


**Fig. 10.** Review-Figure-10: Comparison between Savè supersite observations (grey) and COSMO-ART reference (black), clean (blue) and polluted (red) of (a) net downward shortwave radiation ( $\text{W m}^{-2}$ ), (b) net downwa

C23

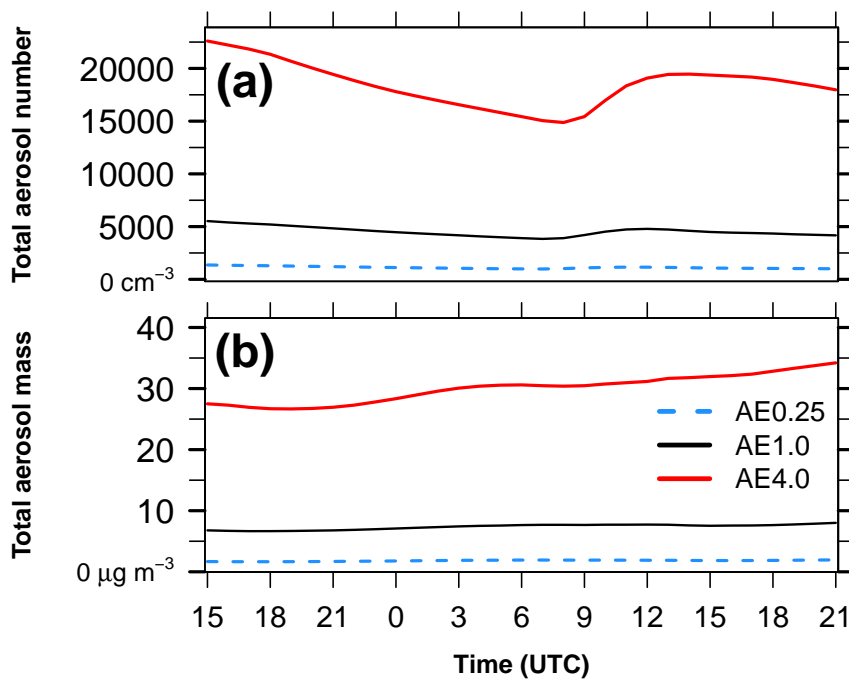


**Fig. 11.** Review-Figure-11: Temporal evolution of median (a) total aerosol number ( $\text{cm}^{-3}$ ) and (b) total aerosol mass ( $\mu\text{g m}^{-3}$ ) in the lowest 2 km AGL over Ivory Coast ( $7.5\text{--}3.0^\circ\text{W}$ ) between 2 July 15 UTC to 3 Ju

C24

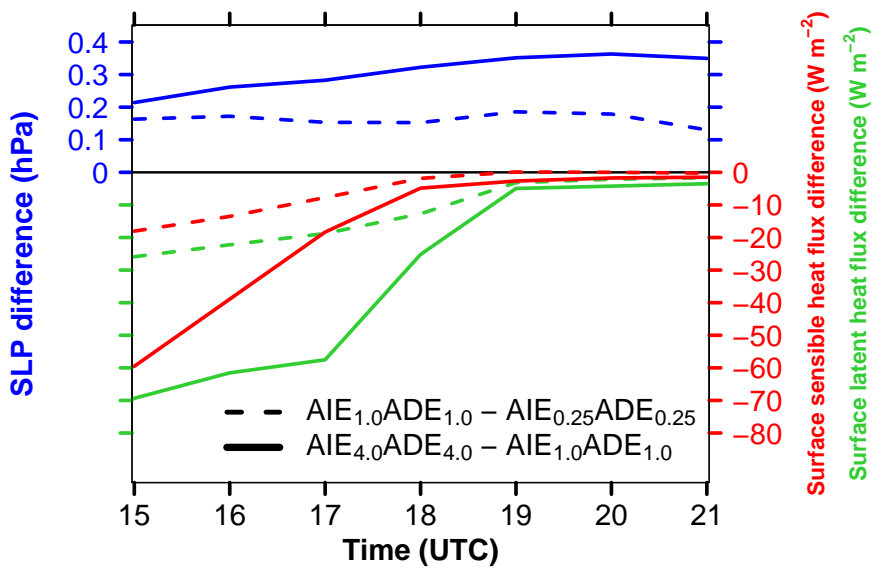


Fig. 12. Review-Figure-12: Temporal evolution of the differences in surface sensible heat flux (red,  $W m^{-2}$ ), surface latent heat flux (green,  $W m^{-2}$ ) and surface pressure (blue, hPa).

C25

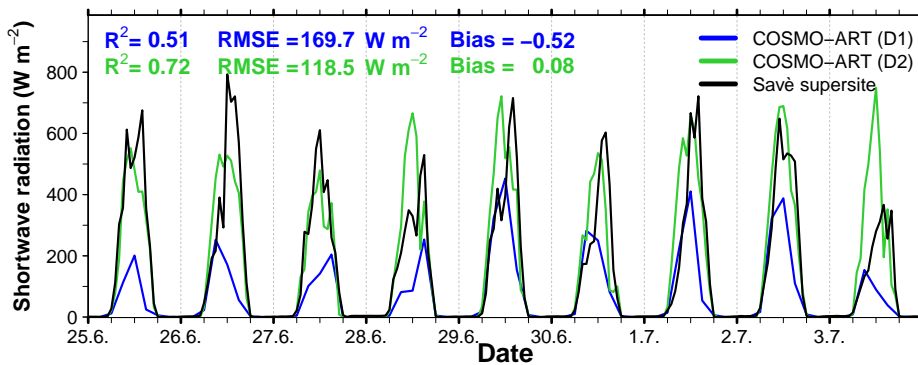
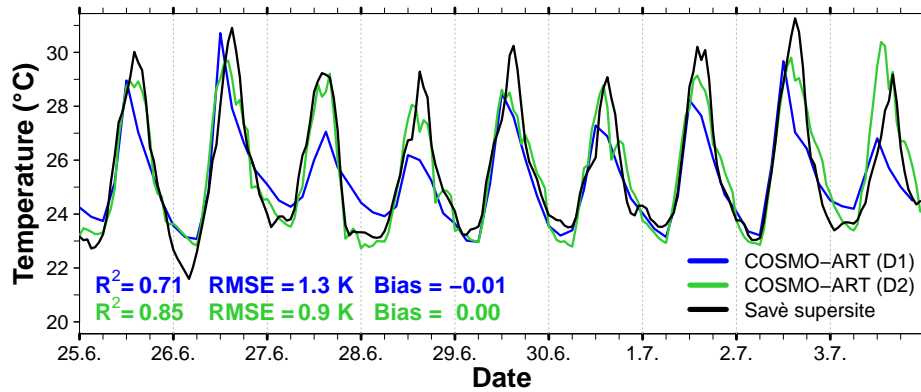


Fig. 13. Review-Figure-13: Temporal evolution of the surface net downward shortwave radiation ( $W m^{-2}$ ) for the nine-day spin-up time (25 June - 3 July 2016) at Savè as observed (black, Energy Balance Station) a

C26



**Fig. 14.** Review-Figure-14: Temporal evolution of the 2 m temperature (°C) for the nine-day spin-up time (25 June - 3 July 2016) at Savè as observed (black, Energy Balance Station) and modeled with COSMO-ART (

C27

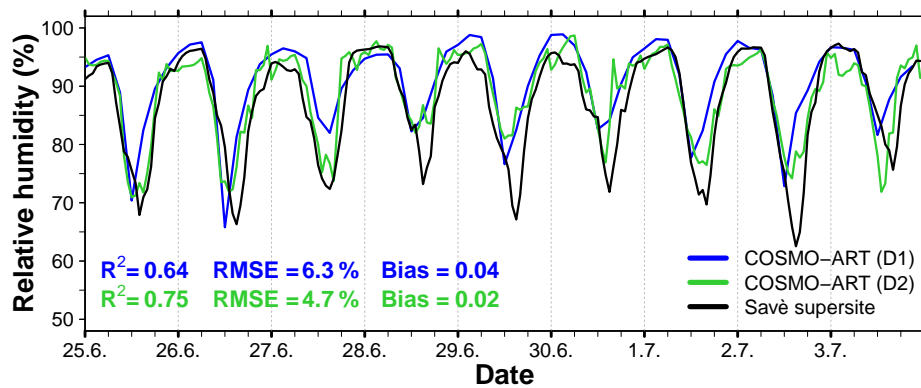


**Fig. 15.** Review-Figure-15: Temporal evolution of the 2 m relative humidity (%) for the nine-day spin-up time (25 June - 3 July 2016) at Savè as observed (black, Energy Balance Station) and modeled with COSMO-A

C28